SUPPLEMENTAL FIGURES TO:

Palaeozoic stromatoporoid diagenesis: a synthesis

Stephen Kershaw[1,2*] Axel Munnecke[3], Emilia Jarochowska[4], Graham Young[5]

[1]Department of Life Sciences, Brunel University, Kingston Lane, Uxbridge, UB8 3PH, UK
[2]Department Earth Sciences Department, The Natural History Museum, Cromwell Road, London, SW7 5BD, UK
[3, 4]GeoZentrum Nordbayern, Friedrich-Alexander University Erlangen-Nuremberg (FAU), Fachgruppe Paläoumwelt, Loewenichstrasse 28, D-91054 Erlangen, Germany; axel.munnecke@fau.de; emilia.jarochowska@fau.de

[5]Manitoba Museum, 190 Rupert Avenue, Winnipeg, Manitoba R3B ON2, Canada; gyoung@manitobamuseum.ca

[*]Corresponding author: Stephen.kershaw@brunel.ac.uk

Fig. S1:

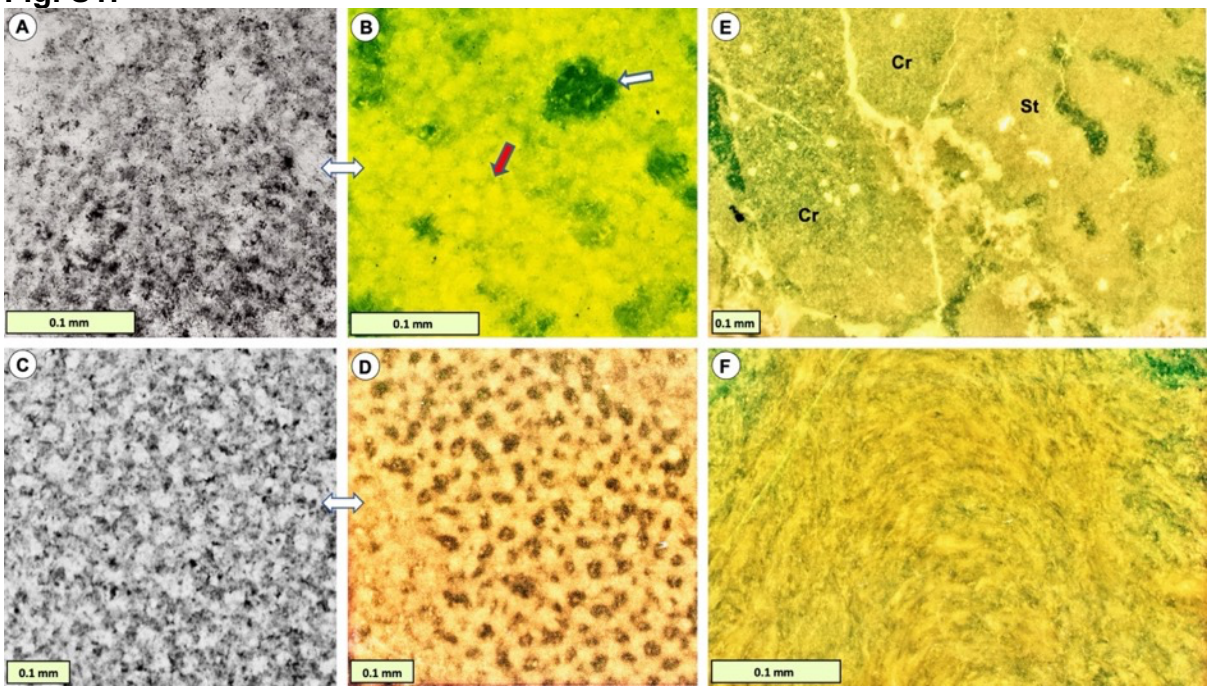

Fig. S1. UV fluorescence images of example stromatoporoids from one locality and facies. **A and B.** TS views of PPL and UV fluorescence images respectively of *Parallelostroma typicum*, a taxon comprising a skeleton composed of a reticulate

network with internal spaces, as well as galleries. In UV light, the stromatoporoid skeleton is light-coloured while intraskeletal space (red arrow) and gallery space (white arrow) are dark-coloured. **C and D.** TS views of PPL and UV fluorescence images respectively of *Plectostroma scaniense*, a taxon composed of a network of long pillars and connecting processes, so that the intervening spaces are very small. In UV light, the skeleton is light-coloured and the non-skeletal space is dark coloured. **E.** UV light view of a small area of grainstone comprising crinoids (Cr) and stromatoporoid (St) fragments. The stromatoporoid shows light-coloured skeleton and dark gallery spaces, and the crinoids show a speckled appearance indicative of very small spaces amongst the skeletal material typical of a crinoid stereom. **F.** UV light view of a VS of the stromatoporoid *Lophiostroma schmidti*, a taxon composed of a layered solid crystal mass, here showing light-coloured crystals with some dark interstices, also visible in normal light images in the main body of this study. See text for discussion. Hemse Group, Ludlow (Silurian), Kuppen biostrome locality, Gotland, Sweden.

Fig. S2:

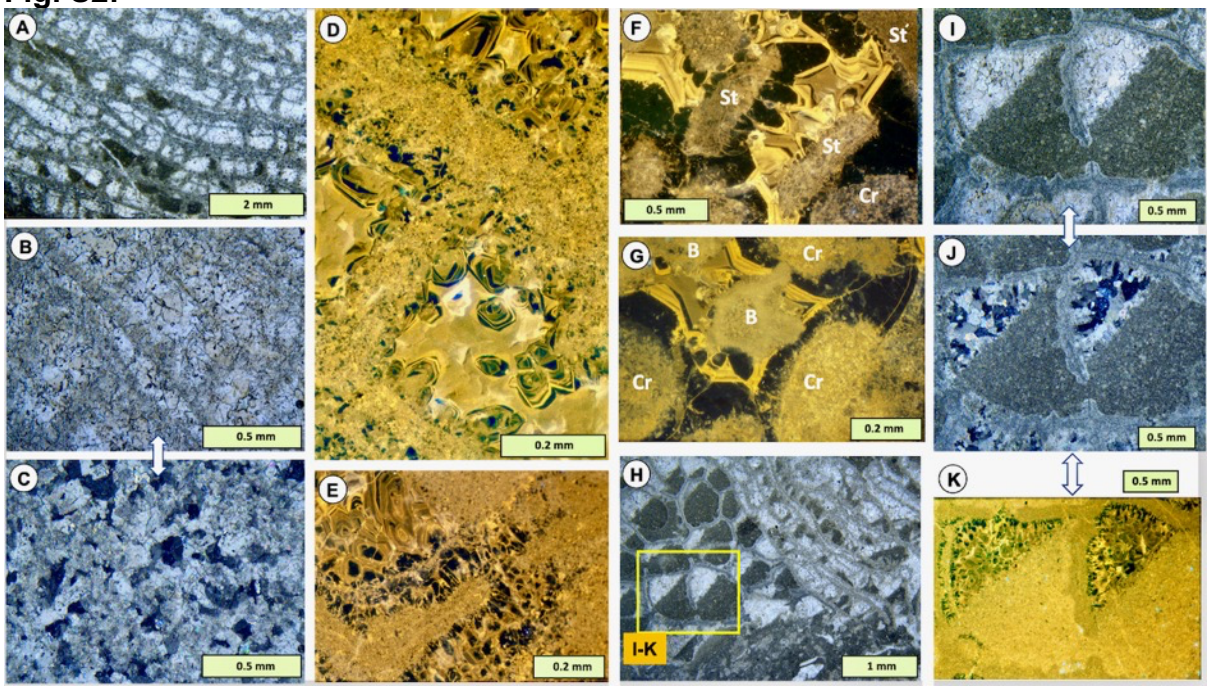

Fig. S2. Thin section and CL comparisons of stromatoporoid taxon *Simplexodictyon yavorskyi* (**A-E**), crinoidal grainstone (**F, G**) and a favositid tabulate (**H-K**), from the same locality and facies. **A.** Vertical section in PPL view showing laminae and pillar structure. **B and C.** Vertical section in PPL and XPL views respectively, demonstrating the FRR structure consists of blocky calcite with poorly developed orientation normal to laminations, contrasting other taxa in the same deposit (Fig. 12). **D and E.** VS and TS respectively of CL view. **F and G.** CL views of crinoidal grainstone showing non-luminescent syntaxial overgrowths on crinoid grains (Cr) while stromatoporoid fragments (St) have smaller calcite crystals. Bright and dull luminescent cements fill the remaining space, and are matched with ferroan calcite in contrast to non-ferroan calcite of the non-luminescent cement (not illustrated). **H.** Vertical section in PPL of favositid tabulate encrusted by the stromatoporoid after a growth interruption event during which micrite accumulated in the coral calices. **I.**

Enlargement of yellow box in H. **J, K.** XPL and CL views respectively of I, showing cement fills in the coral calices, and in K the micrite is more brightly luminescent than the coral. Hemse Group, Ludlow (Silurian), Kuppen biostrome locality, Gotland, Sweden.

Fig. S3:

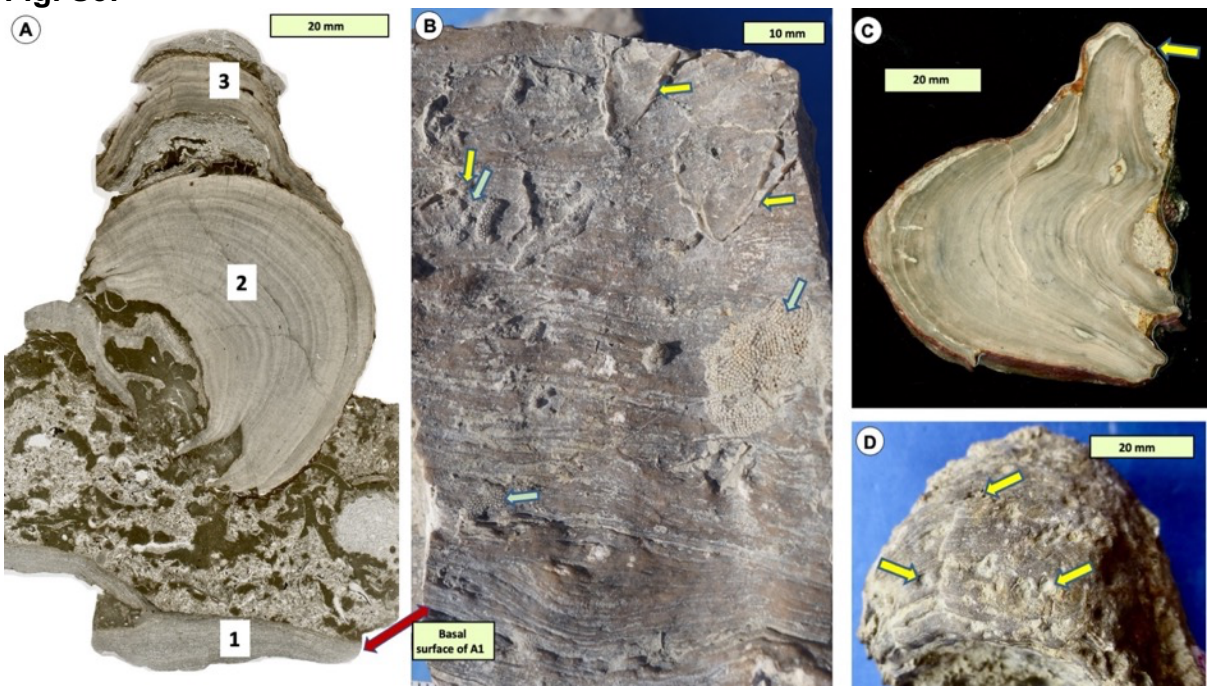

Fig. S3. Evidence of early lithification of clay-carbonate sediment either on or just below the sea floor, affecting burial of stromatoporoids. **A and B (**B is the basal view of stromatoporoid 1). Sequence of events affecting three stromatoporoid specimens. Lowermost stromatoporoid (1) is a laminar growth form and has basal encrusters (B) of brachiopods (yellow arrows) and bryozoans (blue arrows) indicating either a primary cavity, or movement on the substrate to create a secondary cavity. In A, on top of 1 is bioclast-rich micrite with a second stromatoporoid (2) previously bound by early lithification to micrite, preserving its delicate marginal portions; this specimen lies at an oblique angle and is not in growth position. 3 is a second growth consisting of one bryozoan and two stromatoporoids in succession in growth position. **C and D.** For comparison with A and B, are different specimens with evidence of contemporaneous damage to stromatoporoids on the sea floor (yellow arrow in C). D was colonised by numerous boring *Trypanites* (arrows). Upper Visby Formation, Wenlock (Silurian), Ireviken 3 locality, Gotland, Sweden.

Fig. S4:

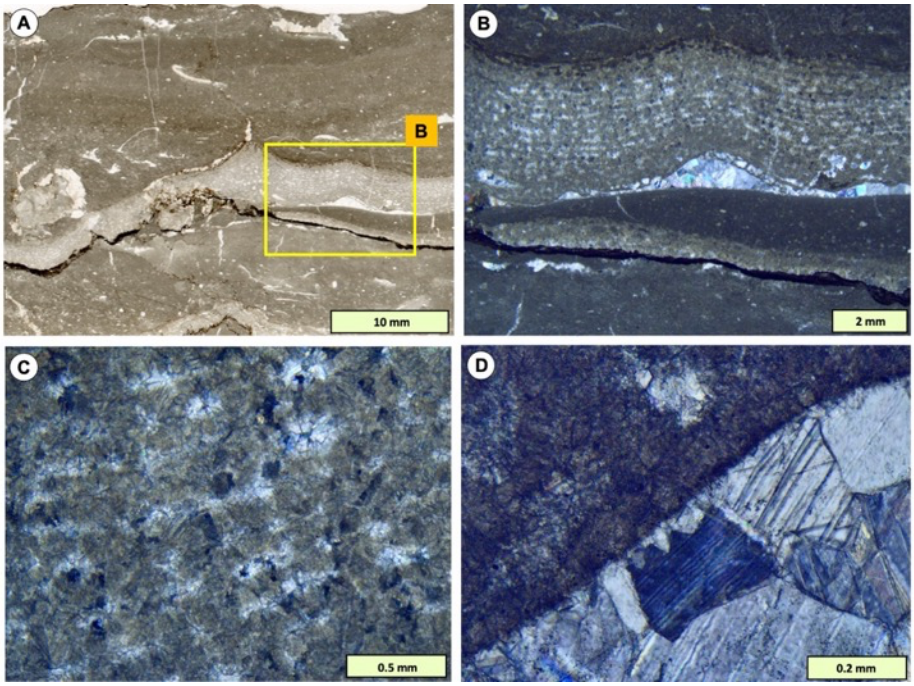

Fig. S4. Vertical section of stromatoporoid with sub-skeletal cavity, Lustin Formation, (Middle Devonian), Tailfer Quarry, southern Belgium. **A.** Vertical whole thin section showing a thin laminar *Stictostroma* (centre across field of view). **B.** XPL view of details of yellow box in A showing a geopetal containing cement. **C.** VS of part of stromatoporoid in XPL showing the overprinting FRIC. **D.** Detail of roof of geopetal where cement abuts against the base of the stromatoporoid, with a thin layer of first generation cement, evidence that the geopetal was cement-filled prior to FRR, so that FRIC did not pass into the geopetal cavity space, a Type 2 cavity (See main body of this study for definitions of Type 1 and Type 2 cavities).

Fig. S5:

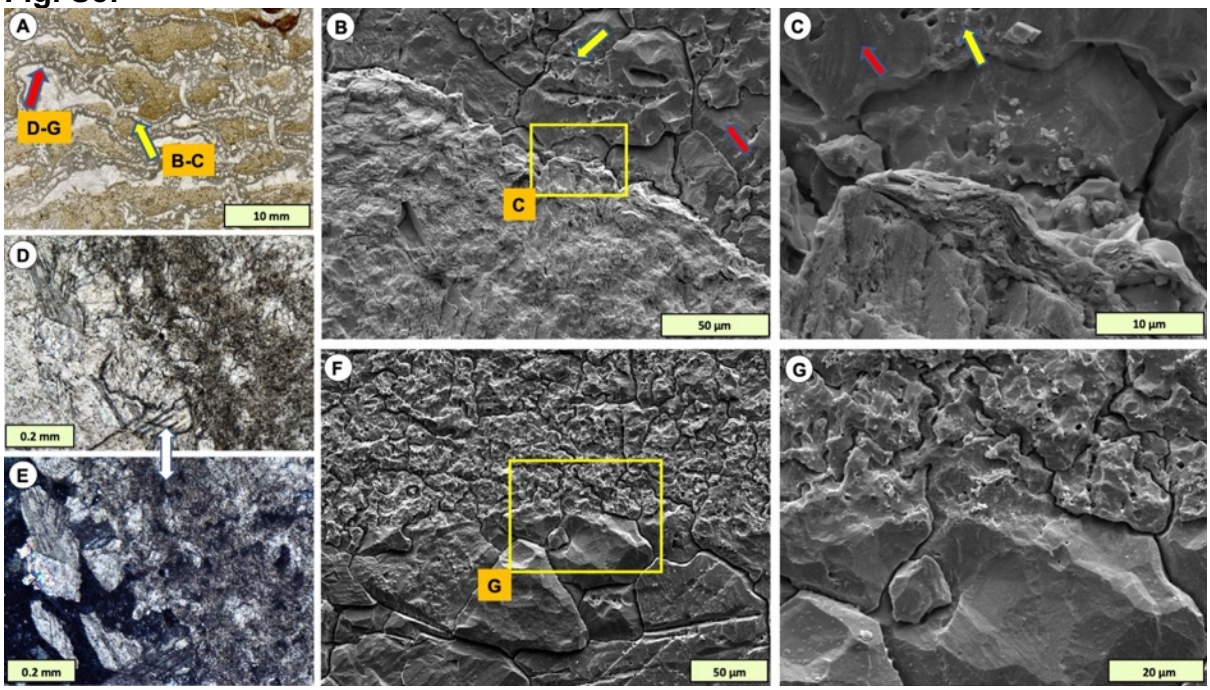

Fig. S5. Subskeletal cavities and cements in an unidentified Devonian stromatoporoid. **A.** Vertical thin section of anastomosing framework of laminar sheets of stromatoporoid creating primary cavities, partly infilled with sediment. Arrows point to examples that are represented in B-G, noting that B-G images are not from those exact locations. **B and C.** SEM secondary electron images showing contact between stromatoporoid base and cavity-filling sediment. There is very minor pressure solution between the stromatoporoid and sediment, but it is clear that crystal boundaries of the recrystallised stromatoporoid skeletal material terminate at the stromatoporoid margin. The stromatoporoid skeletal structure is recognisable as a zone rich in minor pores (yellow arrows), and gallery space is clean sparite (red arrows). In C a dolomite rhomb is visible to the right of the yellow arrow. **D and E.** Thin section of one area in PPL (D) and XPL (E) showing contact between stromatoporoid base and sparite cement in a geopetal cavity. The contact is not absolutely sharp, and is revealed in F and G. **F and G.** SEM secondary electron images of the contact between geopetal cavity sparite cement and base of a laminar sheet of stromatoporoid. Stromatoporoid skeleton is recognised by the zone of minor pores, although this is the basal lamina of the stromatoporoid sheet so there is no gallery space present. Sparite crystal boundaries in the cavity pass up into the stromatoporoid skeleton (Type 2 cavity cement), in contrast to the portions shown in B and C where sediment underlies the stromatoporoid, discussed in the text. Santa Lucia Formation, Emsian (Lower Devonian), Spain; sample donated by Bruno Mistiaen in 1987.

Fig. S6:

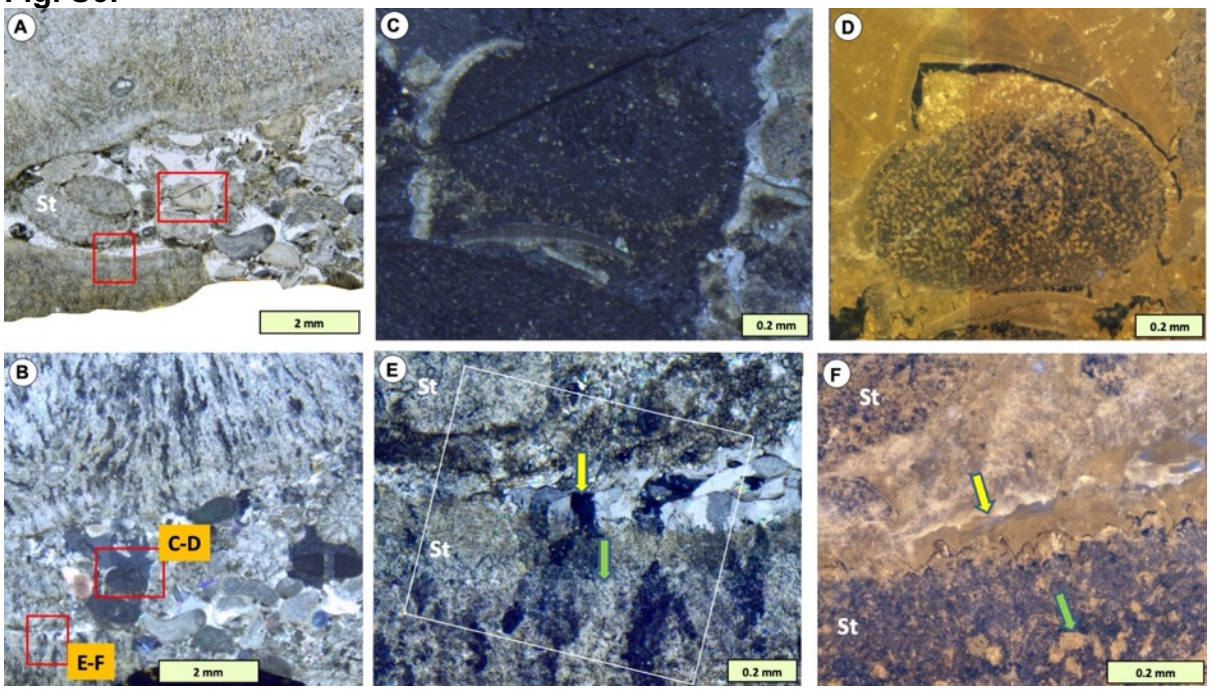

Fig. S6. Stromatoporoids, crinoids and cements. **A and B.** PPL and XPL vertical section views of a stromatoporoid (*Plectostroma scaniense*) with bioclastic grainstone. The stromatoporoid shows FRIC in XPL. Small patches of micrite adhering to grains is evidence of an original packstone fabric with cavity space, possibly formed by sediment dissolution. A stromatoporoid fragment (St) occurs in the bioclastic material. **C and D.** Enlargement of box in A showing a whole crinoid grain (centre) and part of another (bottom) in XPL (C), in extinction, demonstrating syntaxial cement overgrowth; small thin shell fragments (unidentified) are present. D is a CL view showing crinoid stereom and zoned cement overgrowths, mostly dull cement. For C and D, the overgrowth filled the space adjacent to the stromatoporoid. **E.** Stromatoporoid margin and adjacent cement, showing the FRIC passes from the stromatoporoid into the cement (Type 1 cement), evidence that the cement was altered at the same time as the diagenesis that produced FRIC (compare with Fig. 21). The upper stromatoporoid bioclast does not show this relationship with the cement because its surface is blocked by remnant micrite. **F.** Cathodoluminescence view of the oblique box in E showing zoned cements grew on the lower stromatoporoid. In D and F the dull cements are interpreted to represent growth in anoxic conditions, presented as evidence that the FRIC formed below the redox boundary. Stromatoporoid gallery space is filled with dull cement. Yellow and green arrows mark matched points in E and F. Hemse Group limestones, Ludlow (upper Silurian), Snabben locality, Gotland, Sweden.

Fig. S7:

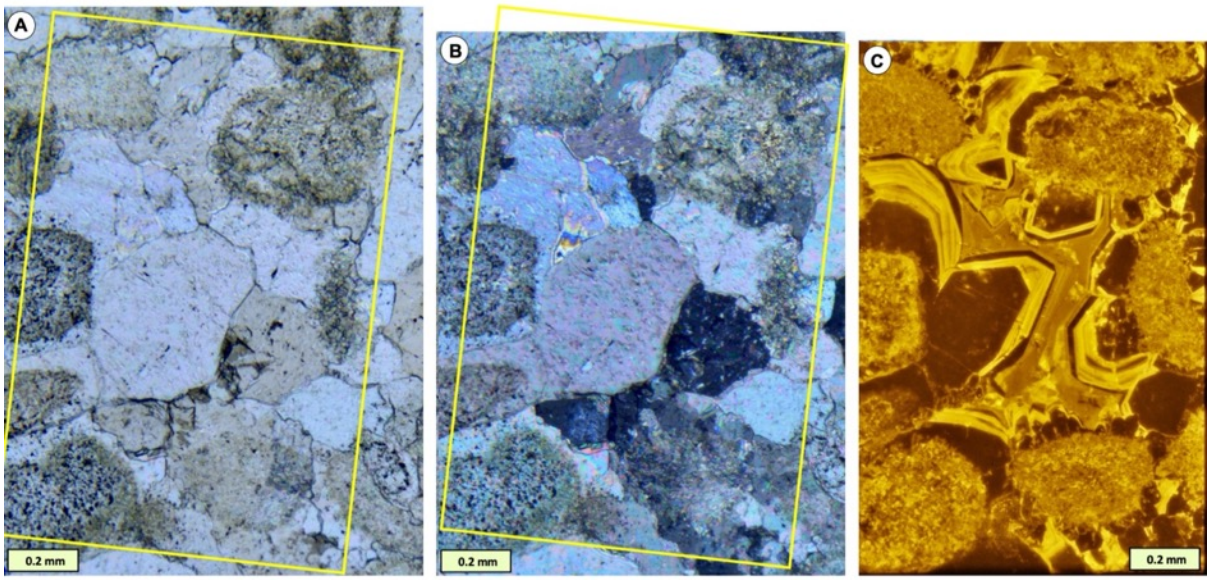

Fig. S7. Crinoidal grainstone to compare with stromatoporoids in the same beds as Figs S1, S2, S6,S9, S10, S11 & S12 in PPL, XPL and CL (A, B, C respectively). These pictures demonstrate: a) the large non-luminescent syntaxial overgrowths in pore spaces, interpreted as early cement, contrasting the smaller amount of such cement in contemporaneous stromatoporoid galleries in other figures; and b) the absence of FRIC in crinoids, contrasting stromatoporoids in other figures, evidence that FRIC does not affect crinoids and is interpreted to have formed later than the syntaxial cements on crinoids. Kuppen biostrome, Hemse Group, Ludlow (Silurian), Kuppen 3 locality, Gotland, Sweden.

Fig. S8:

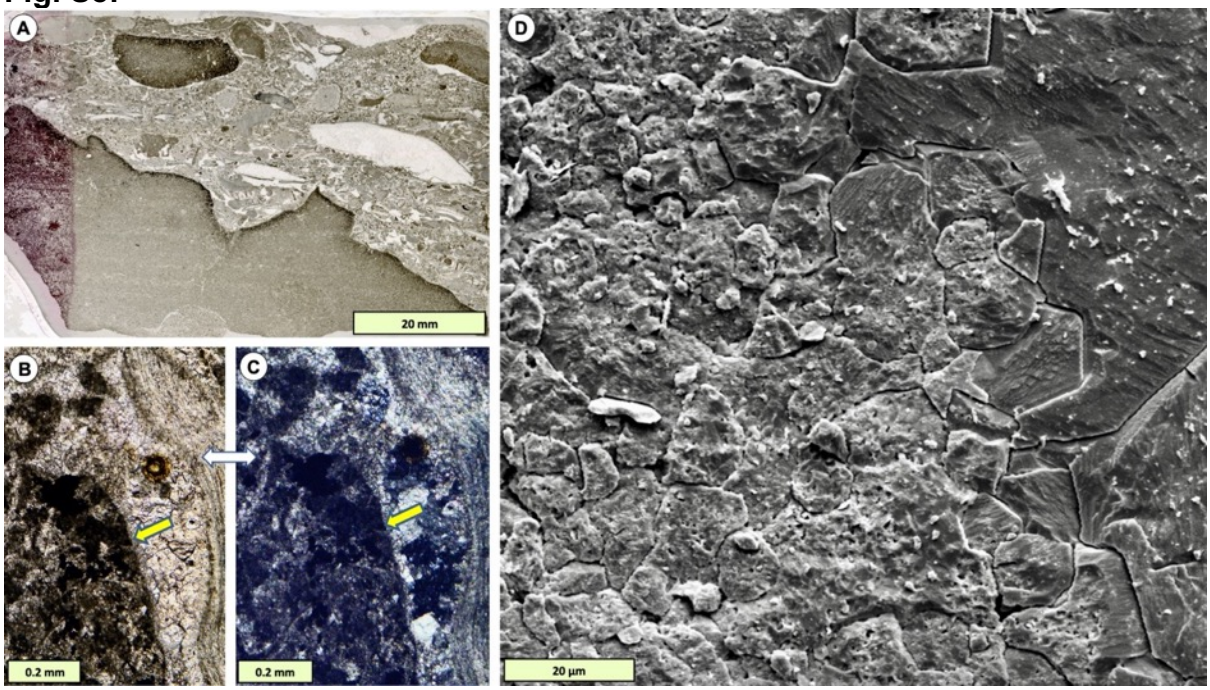

Fig. S8. Contact between eroded lithified limestone surface (likely a hardground) and overlying grainstones (no stromatoporoids) to compare with the margins of stromatoporoids in other figures. **A.** Vertical whole thin section view of eroded surface and sediment. The uppermost edge of the eroded surface is mineralised with unidentified opaque minerals. **B and C.** PPL and XPL thin section views respectively of a small portion of the eroded surface with overlying bioclasts and cement. Yellow arrows mark matched points which are also representative of the location of D, although D is imaged from another part of the specimen. **D.** SEM secondary electron image of vertical section of contact between the micritic limestone below the erosion surface and sparite cement of the overlying grainstone. The contact area shows sparite crystal boundaries pass into the micritic limestone, and are evidence that the sediment was partially recrystallised at the time of the grainstone cementation. The relevance of this to stromatoporoid diagenesis is discussed in the text. Uppermost Högklint Formation, Wenlock (Silurian), Gutevägen locality, Gotland, Sweden.

Fig. S9:

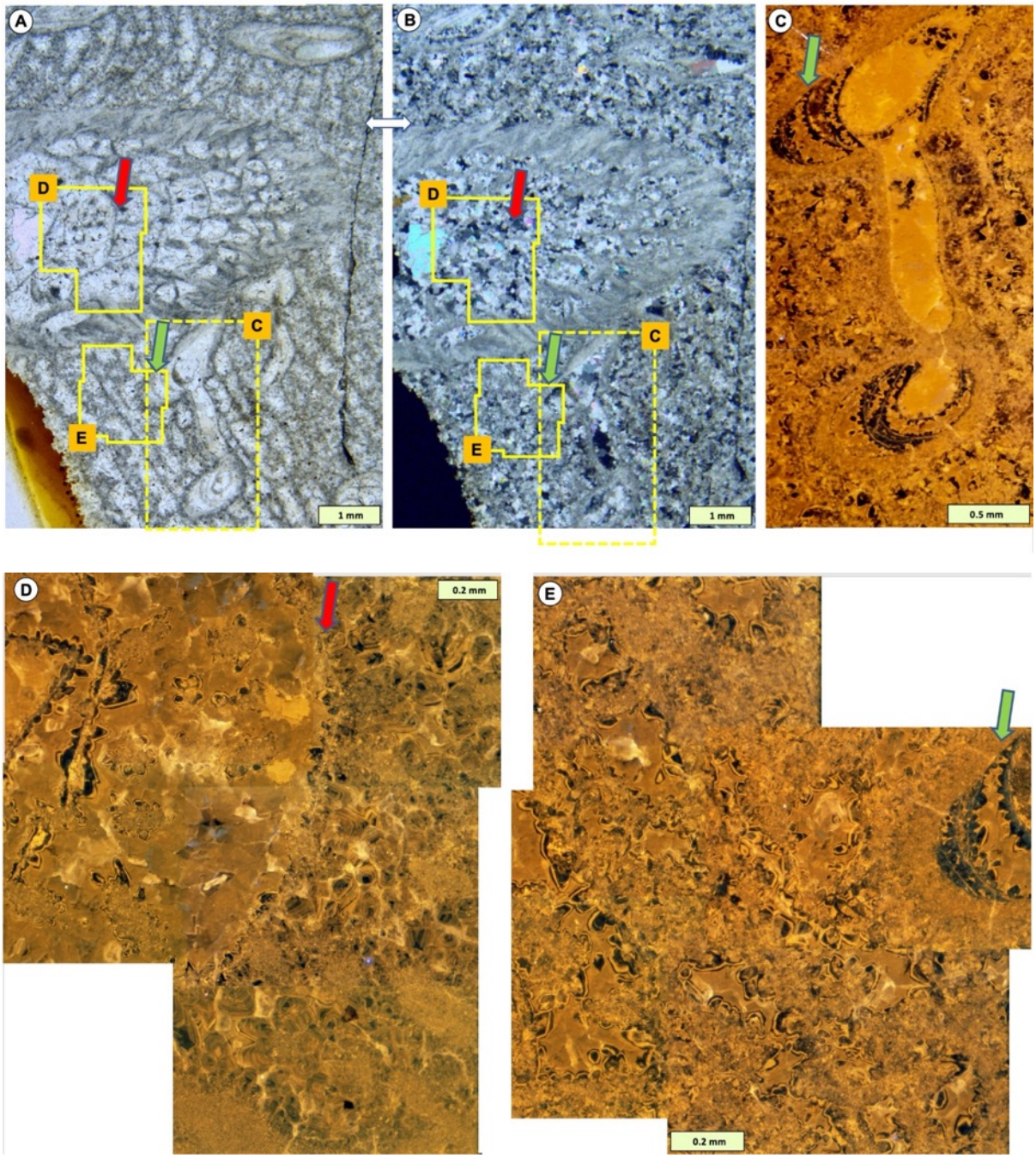

Fig. S9. PPL, XPL and CL views of *Petridiostroma convictum*, with intergrown rugose coral and syringoporid tabulate. **A & B.** PPL (A) and XPL (B), vertical section showing contrast in preservation of the coral and tabulate in contrast to the recrystallised stromatoporoid. **C.** CL view of enlargement of box in A&B, showing the speckled appearance of the stromatoporoid skeleton in contrast to the more even texture of the syringoporid. Green arrow matches location of green arrows in A&B. **D & E.** CL view of enlargements of polygonal boxes in A&B, showing largely dull cement in the calyx of the rugosan (D); and the contrast between speckled CL in the stromatoporoid skeleton and the cement zones in gallery space. Green arrow matches the same points in A-C; red arrow matches same points in A&B. Kuppen biostrome, Hemse Group, Ludlow (Silurian), Kuppen 3 locality, Gotland, Sweden.

Fig. S10:

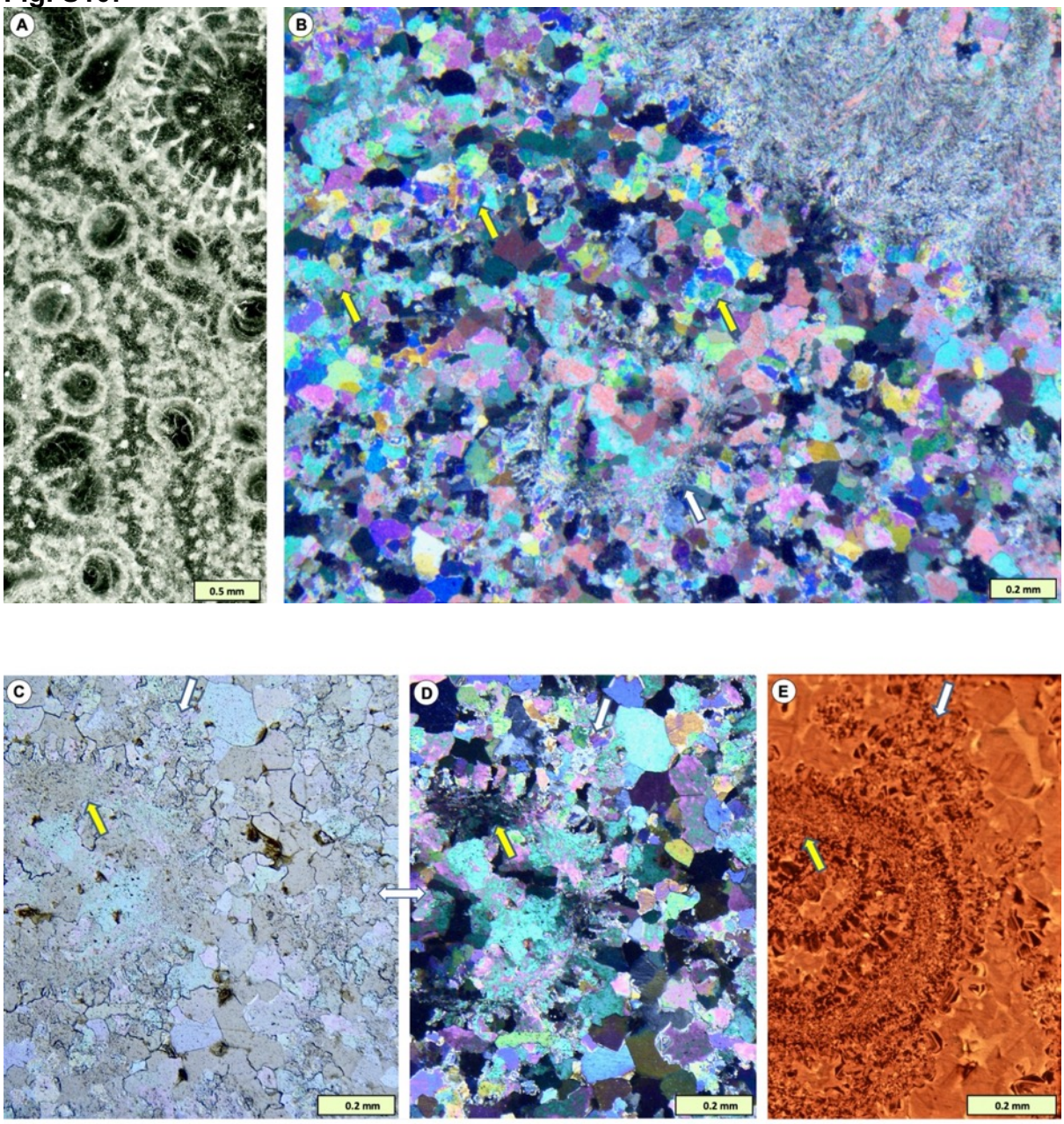

Fig. S10. Views of *Petridiostroma convictum*, with intergrown rugose coral and syringoporid tabulate, showing further detail, following on from Fig. S10. **A.** Negative image of TS thin section in normal light, stromatoporoid skeleton in white, cements in black. **B.** XPL TS view showing part of a rugose coral (upper right), syringoporid tube (white arrow) and altered stromatoporoid skeleton (yellow arrows). Note the circular structure of the syringoporid,partly altered but more easily recognisable than the stromatoporoid skeleton within the sparitic mass of this material. Only the rugose coral is fully distinguishable; this image demonstrates that rugose corals are the best preserved, then syringoporid tabulate is partly altered, and the stromatoporoid skeleton is strongly altered. **C & D.** Superthin section (about 15 microns thick) of matched PPL and XPL views of part of a partly altered syringoporid tube (white arrow) and the altered stromatoporoid skeleton (yellow arrows); note that even in the

syringoporid, the laminated structure is cut across by recrystallisation in XPL view. **E.** CL view of a similar area of the same thin section showing better preservation of the syringoporid compared to the stromatoporoid. Kuppen biostrome, Hemse Group, Ludlow (Silurian), Kuppen 3 locality, Gotland, Sweden.

Fig. S11:

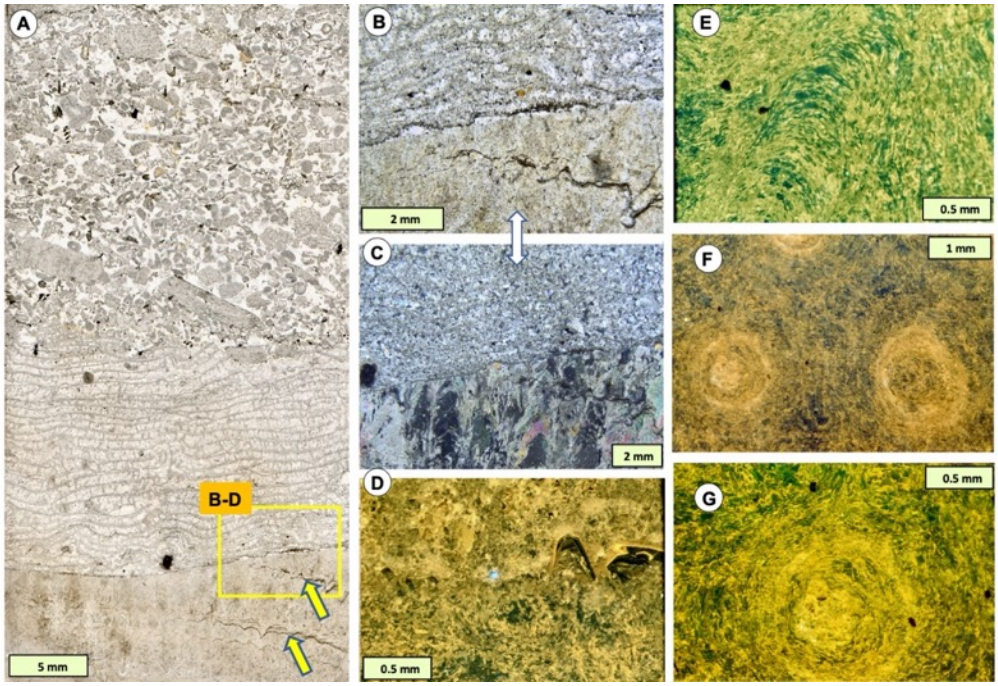

Fig. S11. Thin sections and CL views of two stromatoporoid, plus crinoidal grainstone. **A.** VS PPL view showing *Lophiostroma schmidti* (bottom), with its prominent solid pillar structure. Two small growth interruption surfaces (yellow arrows) emphasise the skeletal structure. Encrusting is *Simplexodictyon yavorskyi* demonstrating prominent laminae and pillars. **B-D.** PPL, XPL and CL views of the same area of thin section, showing *L. schmidti* encrusted by *S. yavorskyi*. The key feature here is that the recrystallised nature of the two stromatoporoids does not pass from one skeleton to the other, showing that they act independently in diagenesis, interpreted in the text as being due to different taxa-related structure. **E-G.** VS (E) and TS (F&G) CL views of *L. schmidti* showing variation of structure picked out by differences in CL, presumably due to changes in skeletal composition as the stromatoporoid grew, for reasons that are unclear. Kuppen biostrome, Hemse Group, Ludlow (Silurian), Kuppen 3 locality, Gotland, Sweden.

Fig. S12.

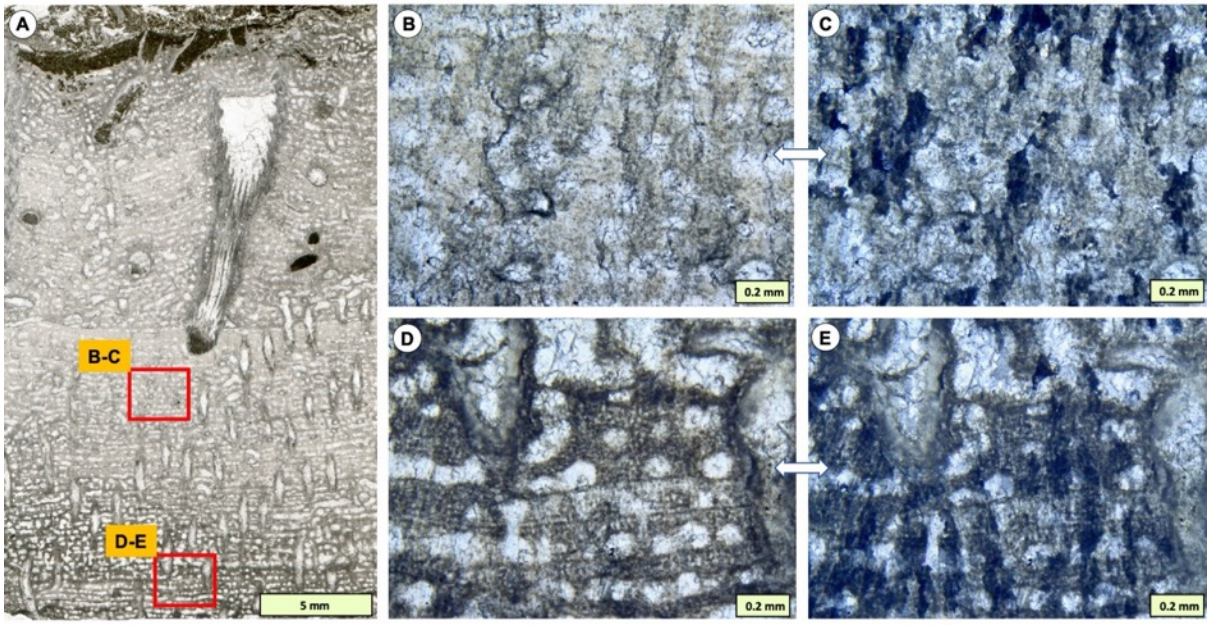

Fig. S12. VS views in PPL and XPL of "*Stromatopora" venukovi* containing intergrown rugose coral and syringoporid tabulate tubes, demonstrating variation of the vertically-orientated recrystallised structure of stromatoporoid preservation in different parts of the same thin section. **A.** General thin section view showing a growth interruption at the top, micrite covered surface and partial micrite penetration into tubes (centre right). **B & C.** Matched areas in PPL (B) and XPL (C) of a poorly preserved area of stromatoporoid skeleton. Even in PPL the overprinting recrystallisation is visible cutting across the skeleton, better seen in XPL. **D & E.** Better preserved skeleton showing its reticulate structure, yet is overprinted by recrystallisation in XPL. Kuppen biostrome, Hemse Group, Ludlow (Silurian), Gotland, Sweden.

Fig. S13:

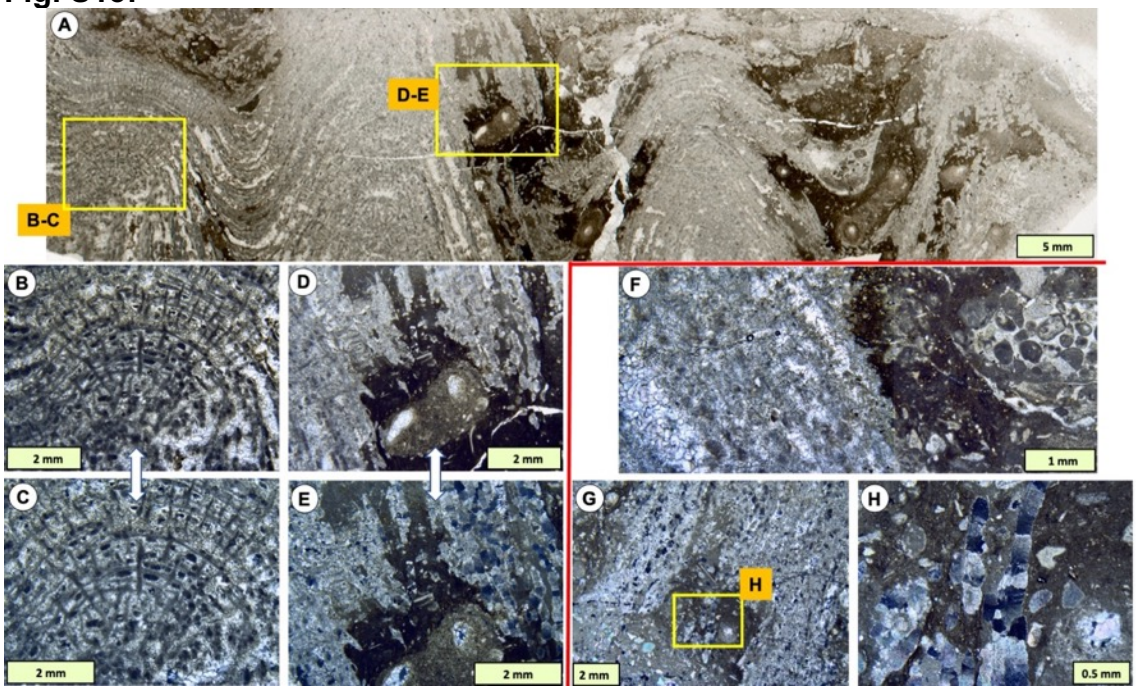

Fig. S13. VS views of thin section of Ordovician stromatoporoid (*Labechia eatoni*, see Kapp & Stearn (1975)) showing variable preservation within the same specimen. **A-E.** are from one thin section, **F-G.** are from a parallel thin section in the same specimen. In E and H the altered structure is very clear. Chazy Group, (Middle Ordovician), Goodsell Quarry, Isle La Motte, Lake Champlain, Vermont, US. Sample donated by Ulla Kapp.

Fig. S14:

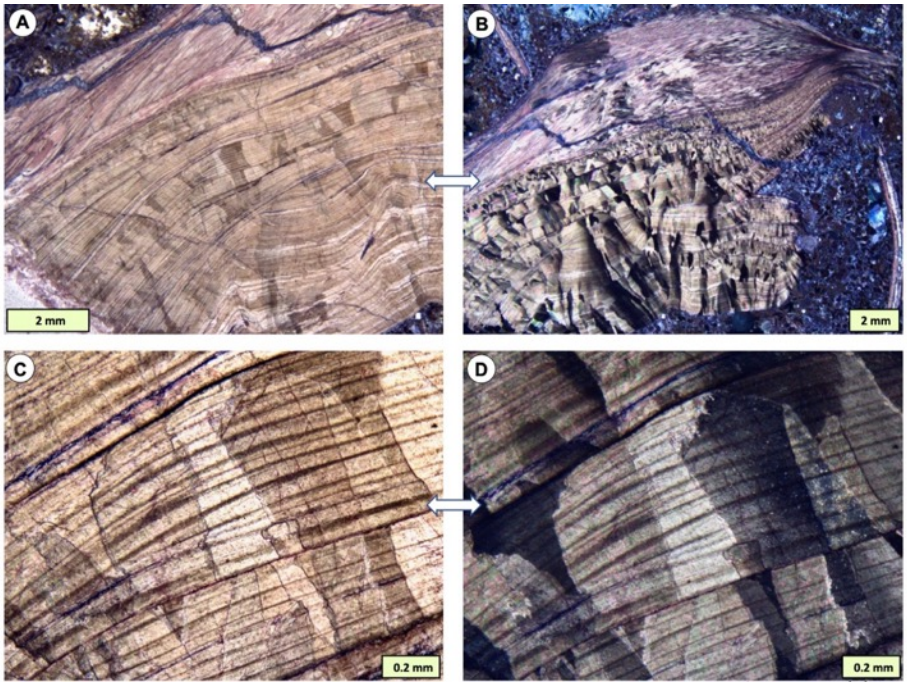

Fig. S14. VS views of variation in bivalve preservation within the same shell. **A & B.** Upper part of the shell is laminated, but lower part shows overprinting recrystallisation similar to the fabrics observed in stromatoporoids. **C & D.** Enlargements showing detail of overprinting recrystallisation. Bathonian, Middle Jurassic, Leckhampton Hill, near Cheltenham, Gloucestershire, UK.

Fig. S15:

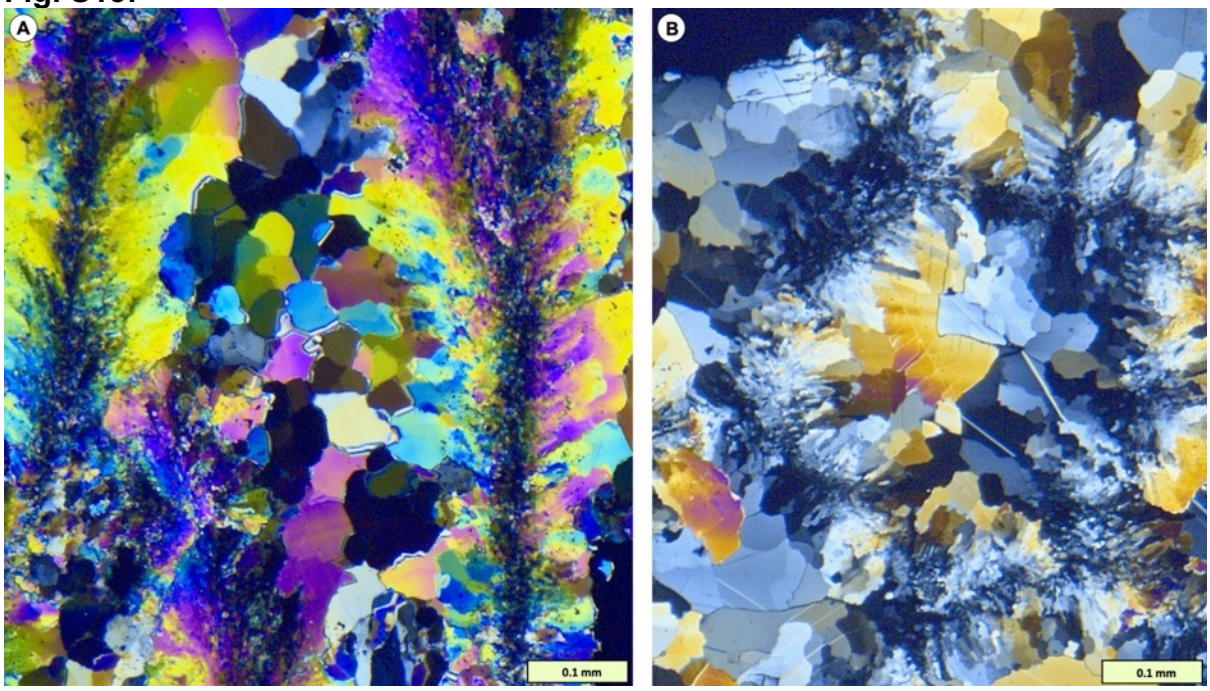

Fig. S15. Microstructure of chaetetid sponges, using very thin sections in cross-polarised light, for comparison with stromatoporoids. **A.** VS showing chevron-like crystalline structure of well-preserved walls of a calicle; **B.** TS showing polygonal

shape of a calicle. Both views show the skeleton developed syntaxial extensions into the calicle space, and the remaining space is filled with sparite. These views are typical of chaetetids, which are better preserved than stromatoporoids shown by the observation that boundaries of cement crystals in the calicles do not pass through the walls, in contrast to stromatoporoids. Note variation of extinction in neighbouring crystals and the passage of extinction through the chaetetid wall indicate that this sample is partially altered but retains its fibrous structure. From a quarry in the Amoret Member of Altamont Limestone Formation, Pennsylvanian subsystem, near Coffeyville, Labette County, Kansas, USA. Thanks to Ron West for facilitating collection of this sample.

Fig. S16:

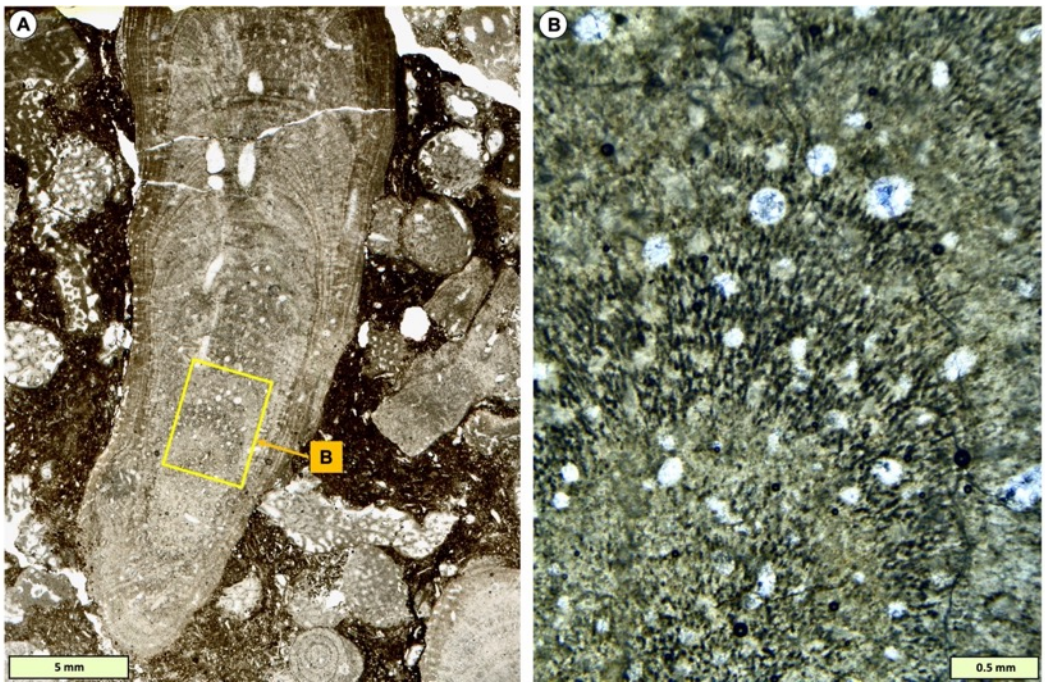

Fig. S16. Thin section views of the dendroid-form stromatoporoid *Stachyodes* sp.; see Stearn (2015d) for taxonomic details. **A.** PPL view of VS of part of *Stachyodes* (vertically-orientated, centre) that is partly oblique showing a portion of the central canal (middle upper part of photo) and some tubules; also typical appearance of the layered structure. In the lower part of the image, the skeleton is sectioned obliquely to transverse, enlarged in B. To left and right of the *Stachyodes* stem are TS views of *Amphipora*, another dendroid-form stromatoporoid that commonly occurs with *Stachyodes*. **B.** XPL view of enlargement of yellow box in A showing a well-preserved example of the dark-coloured pachysteles (vertical skeletal elements) and cross sections of small tubules that altogether typify the skeletal architecture of *Stachyodes*. In the central part of the picture, pachysteles are shown in VS, but at the bottom centre are pachysteles in TS, due to curvature of the structure related to the plane of the thin section. Note that this thin section is quite thick so the structure in B is not all fully focused. From biostromal facies in a bedded limestone sequence, Middle Devonian, Fromelennes, northeastern France.

Fig. S17:

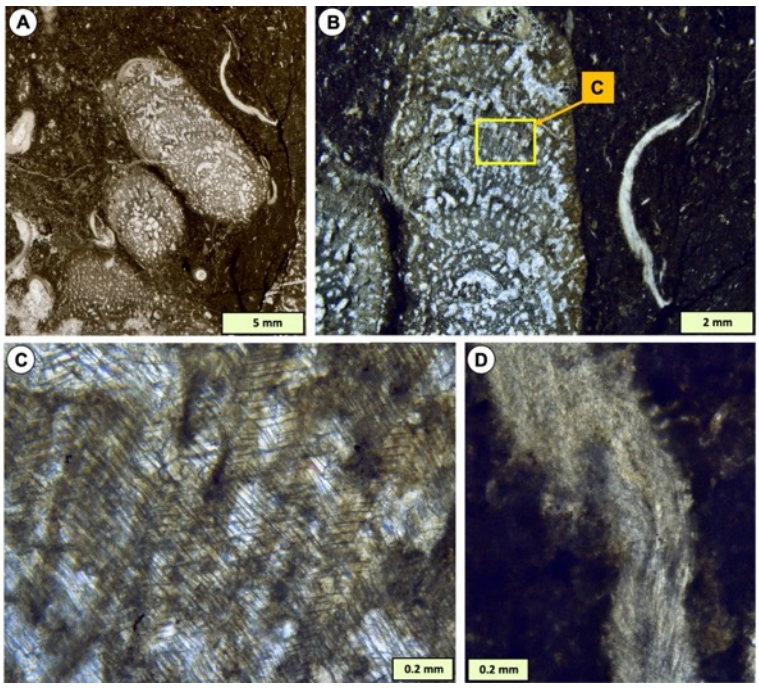

Fig. S17. *Stachyodes* sp. showing recrystallisation of the skeleton. **A.** PPL view of two *Stachyodes* branch pieces in VS (upper centre) and oblique TS (lower centre); a curved brachiopod shell is present in the calcareous mudstone in which the *Stachyodes* is embedded. Other stromatoporoid material at bottom of picture. **B.** Enlargement in XPL showing the complex skeletal architecture of *Stachyodes*. **C.** PPL enlargement of yellow box in B, showing calcite cleavage planes crossing both the skeleton and tubule space, indicating recrystalllisation of the stromatoporoid skeleton. **D.** XPL enlargement of brachiopod in B, showing its well-preserved laminated structure in contrast to the recrystallised stromatoporoid. Back-reef limestone of low-energy environment in calcareous mudstone facies, Givetian, Broadridge Quarry, near Newton Abbot, south Devon, UK.

Fig. S18:

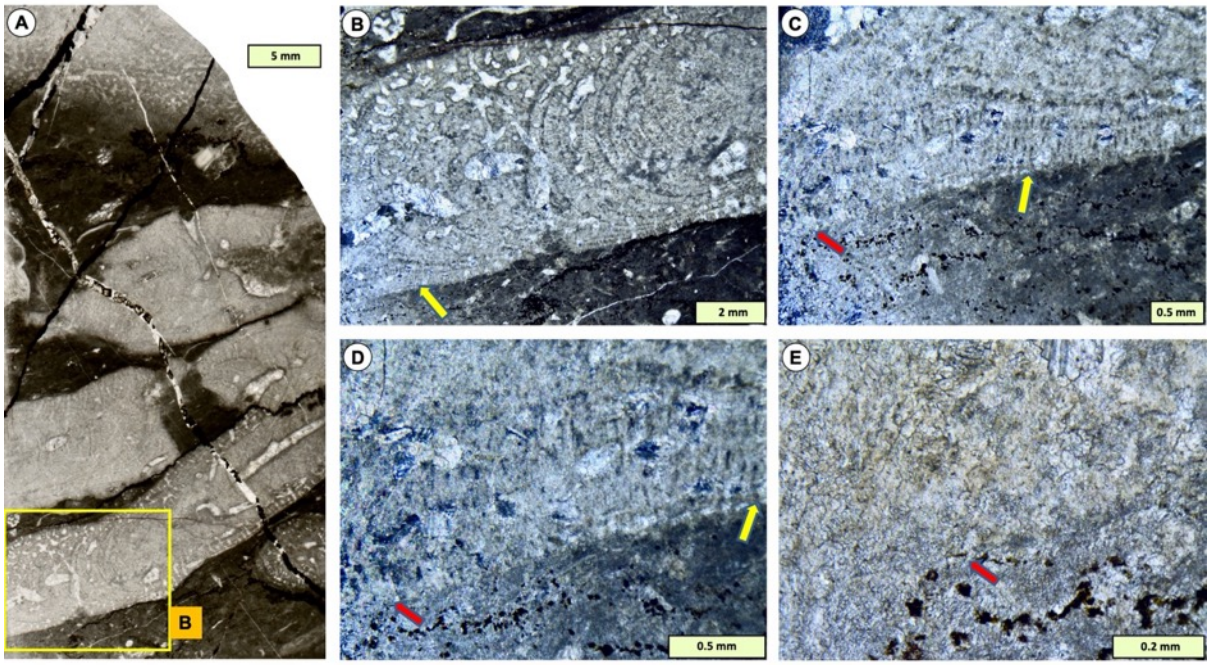

Fig. S18. VS views of *Stachyodes* showing recrystallised structure in sections of varying thickness. **A.** Whole thin section view with four pieces of *Stachyodes* branches lying parallel to each other. The central canal and complex skeletal architecture is visible. **B.** XPL enlargement of yellow box in A, showing, curved laminations and skeletal complexity of the *Stachyodes* skeleton, noting that the thin section thickness decreases towards the bottom left. Yellow arrow shows a matched point with yellow arrows in C and D. **C.** XPL enlargement of lower left corner of B, showing the parallel arrangement of pachysteles in VS, illustrated in Fig. S17, although here they are in a much thinner section. Yellow arrow points at the pachysteles and also matches the sample point in B and D. The red arrow highlights the thinner part of the section where the skeletal structure becomes less easy to distinguish in the recrystallised stromatoporoid skeleton. **D.** XPL enlargement of the lower left corner of C, emphasising the recrystallisation of *Stachyodes*. **E.** PPL enlargement of lower left corner of D. Red arrow (matched to that in B and C) also shows the boundary between stromatoporoid and sediment, that is otherwise difficult to distinguish in this recrystallised stromatoporoid and altered micrite. Givetian, Ashburton Quarry, south Devon, England.